Quantum-mechanical interference effects in the spontaneous-emission spectrum of a driven atom

Shi-Yao Zhu*
Department of Physics, Hong Kong Baptist University, Hong Kong

Lorenzo M. Narducci
Department of Physics, Drexel University, Philadelphia, Pennsylvania 19104

Marlan O. Scully
Department of Physics, Texas A&M University, College Station, Texas 77843
(Received 9 March 1995; revised manuscript received 26 July 1995)

We study the influence of quantum interference on the spontaneous emission from an excited two-level atom when either the atomic upper or lower level is coupled by a coherent field to a third, usually higher-lying, state. In the case of the upper level coupling, destructive quantum interference between two competing decay amplitudes produces a dark line in the emission spectrum, a phenomenon that should not be confused with the well known population trapping, and a narrowing of one of the two side lobes that make up the spectral profile. Quantum interference is absent, instead, in the case of the lower level coupling, and the spectrum modified by the external driving field is just the incoherent superposition of two Lorentzian lines. We suggest a physical interpretation of these results. In addition, we compare the analytic predictions of the simplest nontrivial versions of these models with more realistic but nonanalytic descriptions and show, numerically, that the interference effects persist in the upper level case even when additional complications are taken into account.

PACS number(s): 42.50.Ct, 42.50.Lc

I. INTRODUCTION

The significance of quantum-mechanical interference in spectroscopy has been well documented since the early 1960s [1]. Systems consisting of a ground state, a quasicontinuum of discrete levels, and a true continuum, in particular, have been investigated extensively using Fano's approach or suitable extensions [2], and have yielded among their predictions the emergence of population trapping and holes (or, ideally, zeros) in the fluorescence spectra. More recently, quantum interference phenomena have attracted renewed attention following the discovery of a new class of effects such as optical amplification without population inversion [3], electromagnetically induced transparency [4], and the enhancement of the index of refraction with greatly reduced or, ideally, altogether without absorption [5]. Beside opening the door to possible practical applications which might include the development of new types of lasers, the creation of optical materials with unusual properties, and the design of instrumentation with improved sensitivity [6], quantum-mechanical interference is a fundamental phenomenon, worthy of attention in and of itself, and the source of numerous interesting and counterintuitive manifestations [7].

When a two-level atom decays by spontaneous emission to the ground state, the spectrum of the emitted radiation has a Lorentzian shape as a function of frequency, and a bandwidth that scales with the decay rate of the upper state in the absence of other effects (collisions, external fields, etc.) other than those induced by the field vacuum. If one of the two levels under consideration is coupled to a third state of the atom by a coherent field [8], the spectrum of spontaneous emission may develop structure, such as one normally associates with the emergence of the so-called Autler-Townes doublets [9,10]. In this case quantum interference can be responsible for the appearance of unexpected phenomena.

In this paper we explore the effects of quantum interference on the spontaneous emission spectrum of the atom when either the excited or the ground state is split into Autler-Townes doublets by the action of a coherent field. To be more precise, we wish to compare two different situations. The first corresponds to the setting of Fig. 1(a): the excited atomic state of interest, level 2 in the figure, is coupled by a coherent field to another level of the atom, level

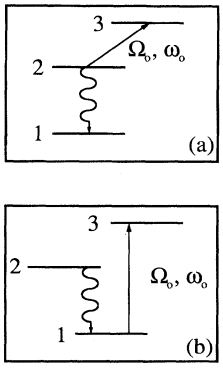

FIG. 1. Schematic representation of the two atomic configurations discussed in this paper; (a) displays the upper level coupling, and (b) the lower level coupling configuration. In both cases Ω_0 denotes the Rabi frequency of the external driving field, and ω_0 its carrier frequency. The wavy line indicates the spontaneous decay process that generates the spectrum of interest.

*Also at the Department of Applied Physics, Shanghai Jiao Tong University, Shanghai 200030, People's Republic of China.

3 in this case [11], and it undergoes spontaneous emission back to the ground state (level 1) as a result of the interaction of the atom with the vacuum. The second situation is illustrated schematically in Fig. 1(b): the atomic ground state is now coupled by the coherent field to another excited atomic level, while level 2, as in the previous case, decays to the ground state by spontaneous emission.

If we ignore, for the moment, the important complications related to the preparation of the initial atomic state, an issue that will be considered in Sec. IV, the main conclusion of our analysis is that, in the first case [Fig. 1(a)] the spontaneous emission spectrum displays a dark feature (a hole in the spectrum) as a result of the destructive interference of competing decay amplitudes, while this dark line is absent in the second case [Fig. 1(b)].

A qualitatively similar prediction was advanced by Agassi some ten years ago [2(a)]. Although the emphasis of Agassi's paper was on the radiative decay properties of atomic states that included continuous bands, the paper also dealt with the spontaneous emission from a set of discrete states with a structure similar to that displayed in our Fig. 1. In the absence of an external applied field, Agassi predicted the emergence of a dark line in the spontaneous emission spectrum which should be best observable when the frequency spacing between the top two levels [levels 1 and 2 in Fig. 2 of Ref. [2(a)]] is comparable to the Einstein spontaneous decay rate. This is, of course, a rather stringent requirement which is avoided with the setting of our paper. In our case the effect is especially pronounced if the driving field is weak and resonant with the 2-3 or the 1-3 transitions, respectively. In fact, for weak, resonant driving fields the dark line splits the usual emission spectrum in two halves, each having the same height and a width which is approximately one-half of the standard value; thus the key signature of the interference effect is the appearance of a split spectrum in the case of Fig. 1(a), a feature which is absent, instead, with the setting of Fig. 1(b) (at least under weak driving field conditions; for sufficiently strong fields two peaks do emerge, but they are a consequence of the large Autler-Townes effect).

With a stronger, but still resonant, driving field the dark feature of the spectrum widens, in line with the expected behavior of the dressed states doublets, whose spacing is controlled by the Rabi frequency of the driving field. In the case of Fig. 1(b), instead, the emission spectrum is the incoherent superposition of two Lorentzian lines; as the strength of the driving fields grows, a dip begins to form which becomes progressively deeper for even stronger driving fields, and the two Lorentzian lines move apart from each other. Thus, also in the second case under study, the spectrum eventually splits into two halves; there are significant differences, however, because not only is the separation of the two spectral components gradual as the driving field strength increases (unlike the first case where the dark line, in principle, is always present as long as the external field is turned on), but also the width of each component matches that of the unperturbed spontaneous emission spectrum, and it is not half as wide.

An additional signature of the different behavior of the two emission processes becomes apparent when the driving field is detuned from the two transition frequencies ω_{32} and ω_{31}, respectively: in the first case, the peak heights of the two spectral components remain equal to one another, but the width of one becomes progressively narrower while the second broadens, as the detuning increases in magnitude. In the second case, the peak height of one component grows and the other decreases, for increasing detuning, while the two linewidths are virtually unaffected.

The above qualitative description provides a useful catalogue of the phenomenology, but it fails to suggest how one can interpret the various aspects of the effect in physical terms. In order to complete this introduction we raise, and hopefully answer, a few questions directed to the issue of the physical interpretation. The first question can be phrased as follows: in what sense are the predicted phenomena a manifestation of quantum interference?

Probably the most direct way to answer is to observe that the application of a resonant field, e.g., between levels 2 and 3 of Fig. 1(a), transforms the previously bare atomic states into new states that are dressed by the (classical) radiation field. Thus, an atom initially excited in level 2 (for example) finds itself in a well defined linear superposition of two dressed states upon application of the driving external field. At the time when the atomic excitation is released spontaneously into the vacuum and the atom decays back to its ground state, the dressed states interfere with each other. After a sufficiently long time, when the emission process has taken its course, the signature of the interference can be found in the presence of a dark line, as described qualitatively above.

Of course, a dark line is a symptom of destructive interference. Thus, the next obvious question is, why destructive? Why not constructive, or perhaps something in between? The answer is that, in fact, the detailed character of the interference depends upon the initial conditions. Constructive interference is also possible and, when this happens, our calculations predict the possibility that, for appropriate values of the parameters, an enhanced emission peak will appear, instead of a dip in the fluorescence spectrum. Intuitively, it is reasonable that one should be able to tailor the character of the interference process by varying the relative complex weights of the interfering histories, but it is not so obvious how to do it. In order to address this issue in some detail, we devote an Appendix to a sketch of a calculation of the spontaneous-emission spectrum starting from an arbitrary initial superposition of the states 2 and 3 of Fig. 1(a), and thus from an arbitrary mixture of the atomic dressed states. The possible existence of positive interference in spontaneous emission, predicted in the Appendix, appears not to have been noticed before.

Perhaps just as obvious is the question, why is quantum interference absent in the case of the lower level coupling? The answer is that in this case, as in the previous one, the decay process can proceed along two paths. In the case of the lower level coupling, however, one can ascertain, in principle, which of the two paths the atom has chosen to decay. This could be done, for example, by monitoring the absorption of a very weak probe tuned between either one of the states of the ground doublet and an excited state elsewhere in the atomic energy spectrum. In the case of the upper level coupling the action of the same probe would unavoidably destroy the initial quantum state of the atom, in the same way as with the standard double slit experiment if one at-

tempted to uncover the path of the proverbial single photon.

In order to identify the key physical features of the predicted behaviors as unambiguously as possible we develop, in Sec. II, simplified models for the two processes in which we retain only the essential ingredients, and ignore both the mechanism by which the atom is placed in its initial excited state and the spontaneous relaxation of the atom from level 3 to lower-lying states. In Sec. III we discuss the results and implications of our calculations and display a few characteristic examples. The influence of the excitation mechanism and of the additional decay processes is considered in Sec. IV, where we use the more general approach based on the regression theorem to derive the spontaneous-emission spectrum along the lines of Refs. [12(a)] and [12(b)]. Section V contains a few general remarks and conclusion comments. This paper also includes an Appendix with the main steps of a calculation in which we extend the analysis of the upper level coupling to more general initial conditions that those considered in Sec. II. This generalization shows that the interference effects need not be always of the destructive type but that, under appropriate conditions, constructive interference is also possible.

II. SIMPLIFIED MODELS AND SPONTANEOUS-EMISSION SPECTRA

In this section we provide an analytic derivation of the spontaneous-emission spectra with the help of the traditional Weisskopf-Wigner approach [13], adapted for the inclusion of an additional coupling mechanism to a higher-lying state in each model. In both cases [Figs. 1(a) and 1(b)] we consider a three-level atom, which is prepared initially in its excited state 2 by an unspecified excitation mechanism (this part of the model will be taken into account explicitly in the more realistic but no longer analytic treatment of Sec. IV). The transition 2-1 is coupled to the vacuum of the electromagnetic field, while the additional transitions 2-3 [see Fig. 1(a)] and 1-3 [see Fig. 1(b)] are induced by a classical field with an assigned Rabi frequency Ω_0. This simplified treatment, as we have already mentioned, omits the spontaneous decay of the excited state 3 to lower-lying states, a feature which will be included in the discussion of Sec. IV. Because the calculation strategy is somewhat different in the two cases for reasons of convenience, we consider each separately and, for ease of nomenclature, we refer to the configuration of Fig. 1(a) as the "upper level coupling," while we refer to that of Fig. 1(b) as the "lower level coupling."

A. Upper level coupling

With reference to Fig. 1(a), the model Hamiltonian has the form

$$H=H_0+H_1^S(t), \tag{2.1}$$

where the unperturbed contribution to Eq. (2.1) is

$$H_0=\sum_{i=1}^{3}\varepsilon_i a_i^\dagger a_i+\sum_j \hbar\omega_j b_j^\dagger b_j \tag{2.2}$$

and the interaction part is

$$H_1^S(t)=i\hbar\sum_j g_j(b_j a_2^\dagger a_1-b_j^\dagger a_1^\dagger a_2) + i\hbar(\Omega_0 e^{-i\omega_0 t}a_3^\dagger a_2-\Omega_0^* e^{i\omega_0 t}a_2^\dagger a_3) \tag{2.3}$$

(the upper index S denotes the Schrödinger picture). The operators $a_i^\dagger, a_i$ are the Fermion creation and annihilation operators for electrons, the index i labels one of the three atomic states of interest, and ε_i denotes the corresponding energy, measured from some convenient reference level; the operators $b_j^\dagger, b_j$, instead, are photon creation and annihilation operators, and the index j labels the momentum and polarization indices of the jth field mode whose frequency is ω_j. The symbol g_j denotes the coupling constant between the atomic transition and the jth mode of the vacuum field, and is given by

$$g_j=\mu\left(\frac{\omega_j}{2\hbar\varepsilon_0 V}\right)^{1/2}, \tag{2.4}$$

where μ is the modulus of the 2-1 transition dipole moment, and V is the quantization volume which will be allowed be become infinite at an appropriate point in the calculation; Ω_0 is the Rabi frequency of the classical driving field, and ω_0 is its carrier frequency which, in this case, is equal or approximately equal to the transition frequency ω_{32}.

We are interested in solving the Schrödinger equation for the driven atom. In the interaction picture this has the form

$$\frac{d}{dt}|\Psi(t)\rangle=-\frac{i}{\hbar}H_1(t)|\Psi(t)\rangle, \tag{2.5}$$

where

$$H_1(t)=e^{iH_0 t/\hbar}H_1^S(t)e^{-iH_0 t/\hbar} =i\hbar\sum_j g_j(e^{-i\delta_j t}b_j a_2^\dagger a_1-e^{i\delta_j t}b_j^\dagger a_1^\dagger a_2) + i\hbar(\Omega_0 e^{-i\Delta_0 t}a_3^\dagger a_2-\Omega_0^* e^{i\Delta_0 t}a_2^\dagger a_3), \tag{2.6}$$

and where the detuning parameters δ_j and Δ_0 are defined by

$$\delta_j\equiv\omega_j-\omega_{21}, \quad \Delta_0=\omega_0-\omega_{32}. \tag{2.7}$$

We assume the state vector of the system at the arbitrary time t to have the form

$$|\Psi(t)\rangle=C_2(t)|\{0\}\rangle|2\rangle+C_3(t)|\{0\}\rangle|3\rangle + \sum_j C_{1j}(t)b_j^\dagger|\{0\}\rangle|1\rangle, \tag{2.8}$$

where $|i\rangle$ $(i=1,2,3)$ is the ith unperturbed stationary state of the atom, $|\{0\}\rangle$ denotes the vacuum of the electromagnetic field, and the initial values of the expansion amplitudes are $C_{1j}(0)=0$, and $C_2(0), C_3(0)$ are arbitrary (apart, of course, for the normalization requirement).

Upon substituting Eq. (2.8) into Eq. (2.5) and after some simple steps, we arrive at the following first-order differential equations for the expansion amplitudes:

$$\frac{d}{dt}C_{1j}(t)=-g_j e^{i\delta_j t}C_2(t), \tag{2.9a}$$

$$\frac{d}{dt}C_2(t)=-\Omega_0^* e^{i\Delta_0 t}C_3(t)+\sum_j g_j e^{-i\delta_j t}C_{1j}(t), \tag{2.9b}$$

$$\frac{d}{dt}C_3(t)=\Omega_0 e^{-i\Delta_0 t}C_2(t), \tag{2.9c}$$

which we can solve along the lines of the traditional approach of Weisskopf and Wigner [13]. Following this procedure, one solves formally Eq. (2.9a) and substitutes the result in Eq. (2.9b). After taking the limit $V\to\infty$, the remaining amplitude equations take the form

$$\frac{d}{dt}C_2(t)=-\Omega_0^* e^{i\Delta_0 t}C_3(t)-\tfrac{1}{2}\gamma C_2(t), \tag{2.10a}$$

$$\frac{d}{dt}C_3(t)=\Omega_0 e^{-i\Delta_0 t}C_2(t), \tag{2.10b}$$

where

$$\gamma=2\pi g^2(\omega_{21})D(\omega_{21}), \tag{2.10c}$$

and $D(\omega_{21})$ is the vacuum density of modes calculated at the atomic transition frequency. In this calculation we have ignored the small vacuum-induced frequency shift in the transition frequency ω_{21}.

Solving the coupled equations (2.10a) and (2.10b) is now a simple matter, and the result of this calculation is

$$C_2(t)=(\sigma^- e^{\lambda^+ t}+\sigma^+ e^{\lambda^- t})e^{i\Delta_0 t}, \tag{2.11a}$$

$$C_3(t)=\Omega_0\left(\frac{\sigma^-}{\lambda^+}e^{\lambda^+ t}+\frac{\sigma^+}{\lambda^-}e^{\lambda^- t}\right), \tag{2.11b}$$

where

$$\sigma^-=\frac{(\lambda^-+\Gamma)C_2(0)+\Omega_0^* C_3(0)}{\lambda^- -\lambda^+}, \tag{2.12a}$$

$$\sigma^+=\frac{(\lambda^++\Gamma)C_2(0)+\Omega_0^* C_3(0)}{\lambda^+ -\lambda^-}, \tag{2.12b}$$

and

$$\lambda^\pm=-\frac{\Gamma}{2}\pm\left[\left(\frac{\Gamma}{2}\right)^2-|\Omega_0|^2\right]^{1/2}, \tag{2.13a}$$

$$\Gamma=\tfrac{1}{2}\gamma+i\Delta_0. \tag{2.13b}$$

It is just as simple to derive an expression for the remaining amplitudes $C_{1j}(t)$; because, however, we are only interested in the asymptotic form of the emission spectrum, we write down only the long-time solutions which we specialize, furthermore, to the initial conditions $C_2(0)=1$, $C_3(0)=0$. The required results are

$$C_2(t\to\infty)=0, \tag{2.14a}$$

$$C_3(t\to\infty)=0, \tag{2.14b}$$

$$C_{1j}(t\to\infty)=\frac{g_j}{\lambda^+-\lambda^-}\left(\frac{\lambda^++\Gamma}{\lambda^-+i(\Delta_0+\delta_j)}-\frac{\lambda^-+\Gamma}{\lambda^++i(\Delta_0+\delta_j)}\right). \tag{2.14c}$$

The spontaneous-emission spectrum, $S(\omega)$, is proportional to the Fourier transform of the field correlation function

$$\langle \mathbf{E}^{(-)}(\mathbf{r},t+\tau)\cdot\mathbf{E}^{(+)}(\mathbf{r},t)\rangle_{t\to\infty} =\langle\Psi(t)|\mathbf{E}^{(-)}(\mathbf{r},t+\tau)\cdot\mathbf{E}^{(+)}(\mathbf{r},t)|\Psi(t)\rangle_{t\to\infty}, \tag{2.15}$$

where, in a finite quantization volume, the positive and negative frequency parts of the electric field operator are given, respectively, by

$$\mathbf{E}^{(+)}(\mathbf{r},t)=i\sum_j\left(\frac{\hbar\omega_j}{2\varepsilon_0 V}\right)^{1/2}\hat{\varepsilon}_j b_j\exp[i(\mathbf{k}_j\cdot\mathbf{r}-\omega_j t)], \tag{2.16a}$$

$$\mathbf{E}^{(-)}(\mathbf{r},t)=[\mathbf{E}^{(+)}(\mathbf{r},t)]^\dagger, \tag{2.16b}$$

and where the asymptotic form of the state vector is

$$|\Psi(t\to\infty)\rangle=\sum_j C_{1j}(\infty)b_j^\dagger|\{0\}\rangle|1\rangle, \tag{2.17}$$

with $C_{1j}(\infty)$ given by Eq. (2.14c). After substituting Eqs. (2.16), (2.17), and (2.14c) into Eq. (2.15), and after carrying out the infinite volume limit, we arrive at the required result

$$S(\omega)\propto|C_{1,\omega}|^2, \tag{2.18}$$

with δ_j replaced by $\delta\equiv\omega-\omega_{21}$ in Eq. (2.14c). The structure of Eq. (2.18), and specifically the dependence of the emission spectrum upon the modulus squared of the sum of two amplitudes, makes it clear by inspection that the detailed spectral shape of the radiated fluorescence is intimately controlled by quantum interference effects. In particular, for $\Delta_0+\delta=0$, the amplitude $C_{1,\omega}$ vanishes identically, thus yielding a dark line in the spectrum at the frequency $\omega=\omega_{31}-\omega_0$, or at the center of the traditional Lorentzian line if the atom is resonantly driven ($\Delta_0=0$). This is one of our main results and it will be discussed and illustrated in greater detail in Sec. III of this paper.

B. Lower level coupling

For the setting illustrated in Fig. 1(b) it is convenient to adopt a slightly different approach [14]. We select

$$H_0=\hbar\omega_{21}a_2^\dagger a_2+\hbar\omega_0 a_3^\dagger a_3+\sum_j\hbar\omega_j b_j^\dagger b_j, \tag{2.19}$$

as the unperturbed Hamiltonian, and

$$H_1^S(t)=\hbar(\omega_{31}-\omega_0)a_3^\dagger a_3+i\hbar\sum_j g_j(b_j a_2^\dagger a_1-b_j^\dagger a_1^\dagger a_2) +i\hbar(\Omega_0 e^{-i\omega_0 t}a_3^\dagger a_1-\Omega_0^* e^{i\omega_0 t}a_1^\dagger a_3) \tag{2.20}$$

as the interaction contribution, where the meaning of the symbols is the same as adopted in Sec. II A. In the interaction picture, the Hamiltonian (2.20) takes the form

$$H_1(t)=H_A+H_B(t), \tag{2.21}$$

where

$$H_A=-\hbar\Delta_0 a_3^\dagger a_3+i\hbar(\Omega_0 a_3^\dagger a_1-\Omega_0^* a_1^\dagger a_3), \quad \Delta_0=\omega_0-\omega_{31} \tag{2.22a}$$

and

$$H_B=i\hbar\sum_j g_j(b_j a_2^\dagger a_1 e^{-i\delta_j t}-b_j^\dagger a_1^\dagger a_2 e^{i\delta_j t}), \tag{2.22b}$$

and the Schrödinger equation is still given by Eq. (2.5), with the new interaction Hamiltonian (2.21). However, instead of expanding the unknown state vector in terms of unperturbed eigenstates of the system, as done in Eq. (2.8), we introduce the dressed atomic eigenstates $|\alpha\rangle$ and $|\beta\rangle$ and the corresponding eigenvalues λ_α and λ_β, defined by

$$H_A|\alpha\rangle=\hbar\lambda_\alpha|\alpha\rangle, \tag{2.23a}$$

$$H_A|\beta\rangle=\hbar\lambda_\beta|\beta\rangle, \tag{2.23b}$$

Their explicit expressions are

$$|\alpha\rangle=\sin\theta|1\rangle+ie^{i\varphi}\cos\theta|3\rangle, \tag{2.24a}$$

$$|\beta\rangle=\cos\theta|1\rangle-ie^{i\varphi}\sin\theta|3\rangle, \tag{2.24b}$$

where

$$\sin\theta=\frac{|\Omega_0|}{\sqrt{\lambda_\alpha^2+|\Omega_0|^2}}, \tag{2.25a}$$

$$\cos\theta=\frac{|\Omega_0|}{\sqrt{\lambda_\beta^2+|\Omega_0|^2}}, \tag{2.25b}$$

$$\Omega_0=|\Omega_0|e^{i\varphi}, \tag{2.25c}$$

and the eigenvalues are given by

$$\lambda_\alpha=-\frac{\Delta_0}{2}+\left(\frac{\Delta_0^2}{4}+|\Omega_0|^2\right)^{1/2}, \tag{2.26a}$$

$$\lambda_\beta=-\frac{\Delta_0}{2}-\left(\frac{\Delta_0^2}{4}+|\Omega_0|^2\right)^{1/2}. \tag{2.26b}$$

At this point we expand the state vector $|\Psi(t)\rangle$ in the form

$$|\Psi(t)\rangle=C_2(t)|2\rangle|\{0\}\rangle+\sum_j[\alpha_j(t)b_j^\dagger|\{0\}\rangle|\alpha\rangle+\beta_j(t)b_j^\dagger|\{0\}\rangle|\beta\rangle], \tag{2.27}$$

and, after some simple calculations, we arrive at the equations of motion for the expansion amplitudes,

$$\frac{d}{dt}C_2(t)=\sin\theta\sum_j g_j e^{-i\delta_j t}\alpha_j(t)+\cos\theta\sum_j g_j e^{-i\delta_j t}\beta_j(t), \tag{2.28a}$$

$$\frac{d}{dt}\alpha_j(t)=-i\lambda_\alpha\alpha_j(t)-g_j\sin\theta e^{i\delta_j t}C_2(t), \tag{2.28b}$$

$$\frac{d}{dt}\beta_j(t)=-i\lambda_\beta\beta_j(t)-g_j\cos\theta e^{i\delta_j t}C_2(t), \tag{2.28c}$$

with the initial conditions $C_2(0)=1$, $\alpha_j(0)=\beta_j(0)=0$ for all values of j.

Next, we solve Eqs. (2.28b) and (2.28c) formally, substitute the results into Eq. (2.28a), and carry out the limit $V\to\infty$, as done in Sec. II A. The result of this calculation is the following equation of motion for the amplitude $C_2(t)$:

$$\frac{d}{dt}C_2(t)=-\pi[\sin^2\theta D(\omega_{21}-\lambda_\alpha)g^2(\omega_{21}-\lambda_\alpha)+\cos^2\theta D(\omega_{21}-\lambda_\beta)g^2(\omega_{21}-\lambda_\beta)]C_2(t). \tag{2.29}$$

In view of the slowly varying nature of the vacuum mode density D and of the coupling parameter g, we can safely let

$$D(\omega_{21}-\lambda_\alpha)\approx D(\omega_{21}-\lambda_\beta)\approx D(\omega_{21}), \tag{2.30a}$$

$$g(\omega_{21}-\lambda_\alpha)\approx g(\omega_{21}-\lambda_\beta)\approx g(\omega_{21}), \tag{2.30b}$$

and arrive at

$$\frac{d}{dt}C_2(t)\approx-\tfrac{1}{2}\gamma C_2(t), \tag{2.31}$$

where the damping rate γ is defined as in Eq. (2.10c). Finally, the asymptotic solutions of the amplitude equations are

$$C_2(t\to\infty)=0, \tag{2.32a}$$

$$\alpha_j(t\to\infty)=g\sin\theta\frac{e^{-i\lambda_\alpha t}}{\frac{1}{2}\gamma-i(\lambda_\alpha+\delta_j)}, \tag{2.32b}$$

$$\beta_j(t\to\infty)=g\cos\theta\frac{e^{-i\lambda_\beta t}}{\frac{1}{2}\gamma-i(\lambda_\beta+\delta_j)}. \tag{2.32c}$$

The long-time correlation function of the spontaneously emitted field is given again by Eq. (2.15), but now the asymptotic form of the state vector is

$$|\Psi(t\to\infty)\rangle=\sum_j[\alpha_j(\infty)b_j^\dagger|\{0\}\rangle|\alpha\rangle+\beta_j(\infty)b_j^\dagger|\{0\}\rangle|\beta\rangle]. \tag{2.33}$$

After substituting Eqs. (2.16a) , (2.16b), and (2.33) into Eq. (2.15) it is a simple matter to show that

$$\langle\mathbf{E}^{(-)}(\mathbf{r},t+\tau)\cdot\mathbf{E}^{(+)}|(\mathbf{r},t)\rangle_{t\to\infty}=\sum_j\frac{\hbar\omega_j}{2\varepsilon_0 V}e^{i\omega_j t}[|\alpha_j(\infty)|^2+|\beta_j(\infty)|^2]. \tag{2.34}$$

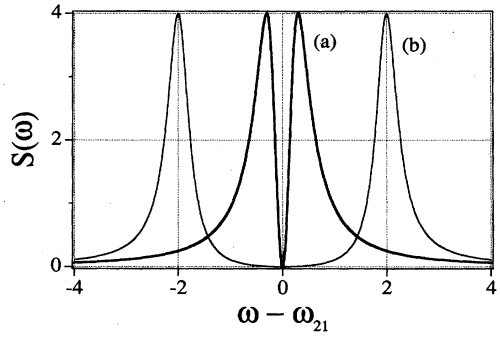

FIG. 2. Spontaneous emission spectrum $S(\omega)$ for the upper level coupling case with $\Delta_0=0$ and (a) $\Omega_0=0.3$, (b) $\Omega_0=2$.

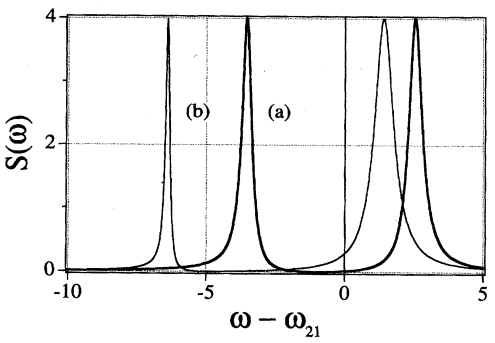

FIG. 3. Spontaneous emission spectrum $S(\omega)$ for the upper level coupling case with $\Omega_0=3$ and (a) $\Delta_0=1$, (b) $\Delta_0=5$.

Thus, in this case, the spectrum of the spontaneously emitted light, after taking the infinite volume limit, becomes

$$S(\omega)\propto|\alpha_\omega(\infty)|^2+|\beta_\omega(\infty)|^2, \tag{2.35}$$

where $\alpha(\infty)$ and $\beta(\infty)$ are given by Eqs. (2.32b) and (2.32c) with δ_j replaced by $\delta\equiv\omega-\omega_{21}$. It is then clear by inspection that $S(\omega)$ is the incoherent sum of two Lorentzian functions each with the same linewidth and that no interference effect is present.

III. DISCUSSION OF THE ANALYTIC RESULTS

While greatly simplified in nature, the models discussed in the preceding section contain the essential physical features that we wish to emphasize in this paper. Thus, Eqs. (2.18) and (2.14c) show that, even a very small amount of coherent mixing of the atomic levels 2 and 3 in Fig. 1(a) is sufficient to induce an interference effect between the spontaneous decay pathways of the dressed excited states. This can be made even more transparent if we rewrite $|C_{1,\omega}|^2$ explicitly as follows:

$$|C_{1,\omega}|^2=g^2\frac{(\Delta_0+\delta)^2}{(\delta^2+\delta\Delta_0-|\Omega_0|^2)^2+\left(\frac{\gamma}{2}\right)^2(\Delta_0+\delta)^2}. \tag{3.1}$$

Equation (3.1) shows by inspection that the spectrum of spontaneous emission develops a dark line centered at $\delta=-\Delta_0$ whose origin can be traced to the negative interference of the two contributing amplitudes.

The structure of the spectral profile is especially simple to analyze when the driving field is resonant with the 2-3 transition. In this case Eq (3.1) shows that the emission line is split symmetrically around $\delta=0$; the two side lobes have equal heights and the maxima are located at $\delta=\pm|\Omega_0|$. Furthermore, the full width at half maximum of each of the side lobes is given approximately by

$$\Delta\omega=\tfrac{1}{2}\gamma\left(1+\frac{|\Omega_0|^2}{(\gamma/2)^2}\right)+O(|\Omega_0|^4), \tag{3.2}$$

in the limit in which $|\Omega_0|\ll\gamma/2$. Hence, it follows that in the presence of a coherent driving field, even with an arbitrarily small amplitude and detuning, the emission spectrum is split into two parts. Two illustrative examples are shown in Fig. 2, under resonance conditions, for two different values of the driving field strength (note that in all the spectral displays, for simplicity, we have set the coupling constant g [see, for example, Eqs. (2.32b) and (2.32c)] equal to unity).

When the driving field is detuned away from the ω_{32} transition frequency the emission spectrum is no longer fully symmetric: the two side lobes continue to have the same peak height, but they are centered at different values of the frequency and have different widths. This effect is illustrated in Fig. 3 for a fixed value of the driving field Rabi frequency and two different positive values of the detuning parameter Δ_0. This figure shows that, while the peak heights of the two spectral components remain the same, an increase of $\Delta_0>0$ broadens the width of the right half of the spectrum and narrows the width of the spectral component on the left of the frequency origin ($\delta=0$). The situation is reversed, relative to the origin of the frequency axis, if the detuning parameter is negative. The derivation of an analytic expression for the two widths of the spectral components is, apparently, a complicated algebraic chore. In the limit in which $|\Delta_0|\gg|\Omega_0|$, the full widths at half maximum of the right and left peaks in Fig. 3 are given approximately by

$$\Delta\omega_R\approx\tfrac{1}{2}\gamma\left(1-\frac{|\Omega_0|^2}{\Delta_0^2}\right), \tag{3.3a}$$

$$\Delta\omega_L\approx\tfrac{1}{2}\gamma\frac{|\Omega_0|^2}{\Delta_0^2} \tag{3.3b}$$

[the subscripts R and L in Eqs. (3.3a) and (3.3b) denote right and left, respectively].

In the case of the lower level coupling [Fig. 1(b)] it is apparent by direct inspection of Eqs. (2.32) and (2.35) that the fluorescence spectrum is just the incoherent sum of two Lorentzian lines, i.e.,

$$S(\omega)\propto\frac{\sin^2\theta}{(\gamma/2)^2+(\delta+\gamma_\alpha)^2}+\frac{\cos^2\theta}{(\gamma/2)^2+(\delta+\gamma_\beta)^2}. \tag{3.4}$$

Each component, one centered at $\delta=-\lambda_\alpha$ and the other at $\delta=-\lambda_\beta$, has a full width at half maximum, γ. On resonance the two lines have the same height, as illustrated in Fig. 4, while out of resonance ($\Delta_0\neq0$) one of the lines be-

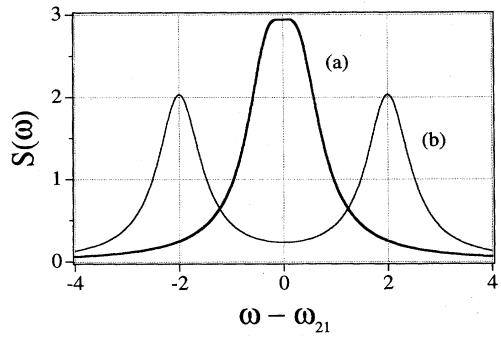

FIG. 4. Spontaneous emission spectrum $S(\omega)$ for the lower level coupling case with $\Delta_0=0$ and (a) $\Omega_0=0.3$, (b) $\Omega_0=2$.

comes progressively more intense relative to the other, as the frequency detuning increases in magnitude (see Fig. 5).

When, under resonance conditions, the strength of the driving field decreases and eventually approaches zero, the frequency spacing between the dressed doublets also vanishes. It is clear that, eventually, the spectra in both the upper and lower coupling schemes will have to approach the usual Lorentzian distribution function. This is true, indeed, but their approach to the Lorentzian shape is very different. In the case illustrated in Fig. 1(a) the spectrum is always split into two side lobes with a dark line in the middle, which disappears only in the absence of the coherent driving field, as suggested by curve *a* in Fig. 2. In the case of the lower level coupling, as the Rabi frequency of the driving field decreases, the dip that separates the two side lobes becomes smaller until, eventually, it disappears when $|\Omega_0|$ becomes of the order of a few tenths of γ, for $\Delta_0=0$ (see curve *a* of Fig. 4).

When the magnitude of the detuning parameter Δ_0 increases, the spontaneous-emission spectra are expected again to approach a Lorentzian shape, as the effect of the driving field becomes less and less pronounced. This continues to be true in both cases, but the approach to the Lorentzian emission line is again very different for the two models.

This is already apparent from the results shown in Figs. 3 and 5, but it become especially obvious if we consider a situation where the driving Rabi frequency is only a small fraction of the spontaneous decay rate. An example is shown in Fig. 6 for the case of the upper level coupling. Taken

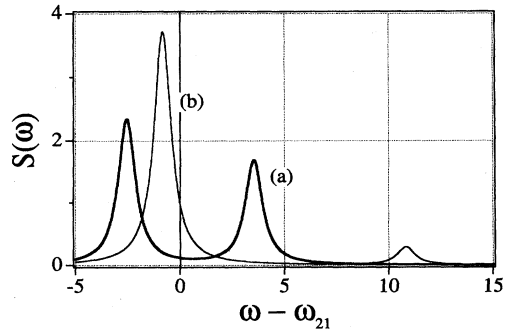

FIG. 5. Spontaneous emission spectrum $S(\omega)$ for the lower level coupling case with $\Omega_0=3$ and (a) $\Delta_0=1$, (b) $\Delta_0=10$.

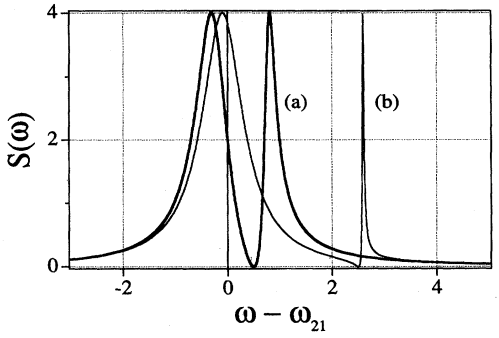

FIG. 6. Spontaneous emission spectrum $S(\omega)$ for the upper level coupling case with $\Omega_0=0.5$ and (a) $\Delta_0=0.5$, (b) $\Delta_0=-2.5$.

together, these results show that, for the configuration of Fig. 1(a) and for increasing values of the detuning, the width of one of the side lobes becomes progressively narrower and the radiated power under this lobe decreases, while the other grows and eventually approaches the standard Lorentzian value. These changes of shape occur with no change in the height of the two components. In the second case the widths of the side lobes remain the same regardless of the value of the detuning, while the peak value of one spectral component decreases and eventually approaches zero.

We must stress that these results apply, strictly speaking, only to the idealized models analyzed in Sec. II, where we have ignored the effects of the pumping mechanisms which are needed to prepare the atoms in their initial state, and the possible influence of additional competing decays, for example the spontaneous decay of level 3. These effects will be described in more detail in the following section.

IV. A MORE REALISTIC MODEL

It is surely not too realistic to expect that the atom can be placed in its initial excited state just at it enters the interaction region. What can be accomplished more easily in a practical setting is to let the interaction of the atoms with the driving fields begin at some arbitrary time, for example when an atom from an atomic beam enters the region occupied by the driving fields, and then to monitor the fluorescence spectrum under steady-state conditions, as done typically in resonance fluorescence studies.

For this purpose we consider an extension of the models illustrated in Figs. 1(a) and 1(b), which includes a second coherent driving field, Ω_1, at or near resonance with the 1-2 transition and also an incoherent pump mechanism characterized by a pump rate W_{12}. The reason for these modifications is to monitor explicitly the effect of the pumping process on the pure interference effect. Furthermore, we also include the remaining spontaneous decay processes at the rates W_{ij}, where i is the starting and j is the terminal level of the decay. The coherent driving field, which is already part of the simplified models, continues to be applied to the same pair of levels and to be denoted by the Rabi frequency Ω_0.

It is no longer practically feasible to handle the extended models by the Weisskopf-Wigner method (state vector method). It is much easier, instead, to describe the atomic

evolution by the standard master equation approach and to derive expressions for the spontaneous emission spectra with the help of the regression theorem [15]. In the calculation of the fluorescence spectra we adopt the procedure discussed in Refs. [12(a)] and [12(b)] but with the help of more convenient assignments of the variables which allow the three-level cascade and V configurations to be described by the same equations [16]. The drawback of the increased generality of the models is that it is no longer possible to identify by inspection the terms responsible for quantum interference, although their presence is obvious from the final numerical results.

We begin with the upper level coupling case. In the presence of a second coherent driving field connecting levels 1 and 2 of Fig. 1(a) the interaction Hamiltonian in the interaction representation takes the form

$$H_1(t)=-\hbar\Delta_1 a_2^\dagger a_2-\hbar(\Delta_0+\Delta_1)a_3^\dagger a_3+i\hbar(\Omega_0 a_3^\dagger a_2 - \Omega_0^* a_2^\dagger a_3)+i\hbar(\Omega_1 a_2^\dagger a_1-\Omega_1^* a_1^\dagger a_2), \tag{4.1}$$

where Δ_0 is defined as in Eq. (2.7), and

$$\Delta_1=\omega_1-\omega_{21}. \tag{4.2}$$

The calculation is based on the master equation and the regression theorem along the lines of Ref. [12(a)]. The relevant equations of motion for the matrix elements of the density operator (in the interaction representation) can be written in the form

$$\frac{d}{dt}\Psi=L\Psi+\mathbf{1}, \tag{4.3}$$

where

$$\Psi_1=\rho_{12},\ \Psi_2=\rho_{13},\ \Psi_3=\rho_{21},\ \Psi_4=\rho_{22},\ \Psi_5=\rho_{23},\ \Psi_6=\rho_{31},\ \Psi_7=\rho_{32},\ \Psi_8=\rho_{33}, \tag{4.4}$$

The matrix L has the explicit form

$$L=\begin{pmatrix} -\Gamma_{12} & -\Omega_0 & 0 & -2\Omega_1^* & 0 & 0 & 0 & -\Omega_1^* \\ \Omega_0^* & -\Gamma_{13} & 0 & 0 & -\Omega_1^* & 0 & 0 & 0 \\ 0 & 0 & -\Gamma_{12}^* & -2\Omega_1 & 0 & -\Omega_0^* & 0 & -\Omega_1 \\ \Omega_1 & 0 & \Omega_1^* & -(W_{21}+W_{23}+W_{12}) & -\Omega_0 & 0 & -\Omega_0^* & (W_{32}-W_{12}) \\ 0 & \Omega_1 & 0 & \Omega_0^* & -\Gamma_{23} & 0 & 0 & -\Omega_0^* \\ 0 & 0 & \Omega_0 & 0 & 0 & -\Gamma_{13}^* & -\Omega_1 & 0 \\ 0 & 0 & 0 & \Omega_0 & 0 & \Omega_1^* & -\Gamma_{23}^* & -\Omega_0 \\ 0 & 0 & 0 & (W_{23}-W_{13}) & \Omega_0 & 0 & \Omega_0^* & -(W_{32}+W_{31}+W_{13}) \end{pmatrix}, \tag{4.5}$$

where

$$\Gamma_{12}=\gamma_{12}+i\Delta_1,\ \Gamma_{13}=\gamma_{13}+i(\Delta_0+\Delta_1),\ \Gamma_{23}=\gamma_{23}+i\Delta_0, \tag{4.6}$$

$$\gamma_{ij}=\tfrac{1}{2}\sum_{k=1}^{3}(W_{ik}+W_{jk}), \tag{4.7}$$

with $W_{ii}=0$ $(i=1,2,3)$, and the inhomogeneous vector $\mathbf{I}$ has nonzero components

$$I_1=\Omega_1^*,\ I_3=\Omega_1,\ I_4=W_{12},\ I_8=W_{13}. \tag{4.8}$$

The required spectrum is proportional to the Fourier transform of the two-time correlation function

$$\Gamma^{(1)}(t_1,t_0)=\langle P^{(-)}(t_1)P^{(+)}(t_0)\rangle, \tag{4.9a}$$

where

$$P^{(+)}=\mu_{12}a_1^\dagger a_2,\quad P^{(-)}=[P^{(+)}]^\dagger. \tag{4.9b}$$

Equation (4.9a) must be calculated in steady state, i.e., under the double limit

$$t_0,t_1\to\infty,\ t_1-t_0\equiv\tau>0, \tag{4.10}$$

where τ is arbitrary. Following the same procedure as described in Ref. [12(a)] leads to the result

$$\Gamma^{(1)}(\tau)=\mu_{12}^2 e^{i\omega_1\tau}\left[(e^{L\tau})_{11}\Psi_4(\infty)+(e^{L\tau})_{12}\Psi_5(\infty)+\int_0^\tau d\tau'\sum_{j=1}^{8}(e^{L(\tau-\tau')})_{1j}I_j\Psi_3(\infty)\right], \tag{4.11}$$

where

$$\Psi_i(\infty)=-\sum_{j=1}^{8}(L^{-1})_{ij}I_j \tag{4.12}$$

denotes the ith stationary matrix element of the density operator, according to the notations introduced in Eq. (4.4).

After elimination of the coherent part, the spectrum of the radiated fluorescence is given by

$$S(\omega)=\mathrm{Re}\hat{\Gamma}^{(1)}_{\mathrm{incoh}}(z)|_{z=i\omega}, \tag{4.13}$$

where $\hat{\Gamma}^{(1)}_{\text{incoh}}(z)$, the so-called incoherent part of the Laplace transform of $\Gamma^{(1)}(\tau)$, has the explicit form

$$\hat{\Gamma}^{(1)}_{\text{incoh}}(z)=M_{11}(z-i\omega_1)\Psi_4(\infty)+M_{12}(z-i\omega_1)\Psi_5(\infty)+\sum_{j=1}^{8}N_{1j}(z-i\omega_1)I_j\Psi_3(\infty), \tag{4.14}$$

and where

$$M_{ij}(z)=[(z-L)^{-1}]_{ij}, \tag{4.15a}$$

$$N_{ij}(z)=[L^{-1}(z-L)^{-1}]_{ij}. \tag{4.15b}$$

We note that, in the absence of a second driving field, we must replace formally ω_1 with ω_{21}. Furthermore, if $\Omega_1=0$, we also have $\Psi_3(\infty)=0$ so that the integral term in Eq. (4.11) is absent, and no subtraction of the coherent Rayleigh scattering is needed (of course).

For the case of the lower level coupling the interaction Hamiltonian is given by

$$H_1(t)=-\hbar\Delta_1 a_2^\dagger a_2-\hbar\Delta_0 a_3^\dagger a_3+i\hbar(\Omega_0 a_3^\dagger a_1-\Omega_0^* a_1^\dagger a_3)+i\hbar(\Omega_1 a_2^\dagger a_1-\Omega_1^* a_1^\dagger a_2). \tag{4.16}$$

With the same assignment of the components of the vector Ψ as given by Eq. (4.4), the new matrix L takes the form

$$L=\begin{pmatrix}
-\Gamma_{12} & 0 & 0 & -2\Omega_1^* & 0 & 0 & -\Omega_0^* & -\Omega_1^* \\
0 & -\Gamma_{13} & 0 & -\Omega_0^* & -\Omega_1^* & 0 & 0 & -2\Omega_0^* \\
0 & 0 & -\Gamma_{12}^* & -2\Omega_1 & -\Omega_0 & 0 & 0 & -\Omega_1 \\
\Omega_1 & 0 & \Omega_1^* & -(W_{21}+W_{23}+W_{12}) & 0 & 0 & 0 & (W_{32}-W_{12}) \\
0 & \Omega_1 & \Omega_0^* & 0 & -\Gamma_{23}^* & 0 & 0 & 0 \\
0 & 0 & 0 & -\Omega_0 & 0 & -\Gamma_{13}^* & -\Omega_1 & -2\Omega_0 \\
\Omega_0 & 0 & 0 & 0 & 0 & \Omega_1^* & -\Gamma_{23} & 0 \\
0 & \Omega_0 & 0 & (W_{23}-W_{13}) & 0 & \Omega_0^* & 0 & -(W_{32}+W_{31}+W_{13})
\end{pmatrix}, \tag{4.17}$$

where

$$\Gamma_{12}=\gamma_{12}+i\Delta_l,\quad \Gamma_{13}=\gamma_{13}+i\Delta_0,\quad \Gamma_{23}=\gamma_{23}+i(\Delta_1-\Delta_0), \tag{4.18}$$

and the inhomogeneous vector $\mathbf{I}$ has nonzero components

$$I_1=\Omega_1^*,\quad I_2=\Omega_0^*,\quad I_3=\Omega_1,$$

$$I_4=W_{12},\quad I_6=\Omega_0,\quad I_8=W_{13}. \tag{4.19}$$

With the chosen notations, the fluorescence spectrum is given again by Eqs. (4.13), (4.14), and (4.15).

Of course, the inclusion of the additional driving fields and decay pathways (and, possibly, also the incoherent pump processes) changes the structure of the ideal spectra discussed in Secs. II and III, but the differences are mainly quantitative unless the added decay rates become too large in comparison with the Rabi frequency Ω_0. With a careful selection of the atomic levels it should be possible to display evidence of the essential differences between the upper and lower level coupling, at least as far as quantum interference effects are concerned. As an example we show the fluorescence spectra from two identical sets of atoms with the same driving field Ω_0 applied to the transition 2-3 of Fig. 1(a) and 1-3 of Fig. 1(b). In both cases a second weaker field is responsible for creating the initial state of excitation whose spontaneous emission yields the calculated spectrum. The results are shown in Figs. 7 and 8, respectively, and are certainly quite different from each other in spite of the fact that all the parameters of the problem are identical in the two cases. Also, the qualitative similarity with the results shown in Figs. 2 and 4 should be immediately apparent, in support of our previous claims to the effect that the inclusion of additional complications should not alter the appearance of interference effects to the point of making them unobservable.

V. DISCUSSION AND CONCLUSIONS

The fluorescence spectrum of a two-level atom can undergo significant modifications in the presence of an external driving field. This has been well known since the late 1960s

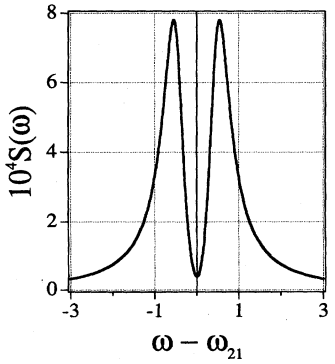

FIG. 7. Spontaneous emission spectrum $S(\omega)$ for the upper level coupling case with $\Omega_0=0.5$, $\Omega_1=0.03$, $\Delta_0=\Delta_1=0$, $W_{21}=1$, $W_{32}=0.2$, and $W_{31}=0.02$.

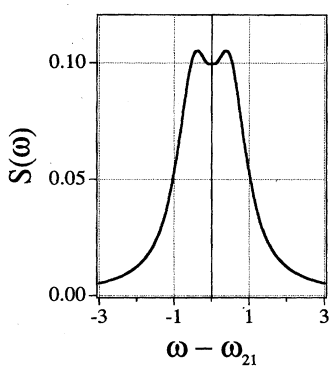

FIG. 8. Spontaneous emission spectrum $S(\omega)$ for the lower level coupling case with $\Omega_0=0.5$, $\Omega_1=0.03$, $\Delta_0=\Delta_1=0$, $W_{31}=0.02$, $W_{21}=1$, and $W_{32}=0.2$.

from the work of several authors [17] who explored the effect of a coherent field tuned close to or at resonance with the two-level transition of interest. In this work we have analyzed the effect of an external driving field which couples either the upper or lower atomic transition to a third level in the atom's energy-level structure. The main result of our analysis is that, in the case of the upper level coupling, quantum interference effects produce a "hole" in the spontaneous emission spectrum, an effect which is absent (at least for weak driving field Ω_0) in the case of the lower level coupling where interference plays no role.

Quantum interference effects are the source of numerous other observed spectral features in both the emission and the absorption spectra of driven multilevel atoms. The predicted and observed line narrowing in the spontaneous emission spectrum of a three-level atom in a V configuration [12a] is one such example. Another is the population trapping [7] which can be made especially obvious in another kind of three-level atom, the so-called $\wedge$ system. Although population trapping shares common physical roots with the dark line feature of the fluorescence spectrum, it should not be confused with the effect discussed in this paper.

Under population trapping conditions [we are thinking especially of a $\wedge$ system, such as discussed in Ref. [7(b)]], there is no absorption from the lowest two levels to the top excited state. Thus the excited state stays empty in steady state, and no light is emitted spontaneously at any frequency. Furthermore, the cancellation of absorption, a purely destructive interference phenomenon, is a coherent process which is degraded by incoherent effects. In our case, instead, quantum interference leads to the cancellation of spontaneous emission at certain frequencies; in addition the process is intrinsically incoherent in nature.

In a sense population trapping and the kind of quantum interference effect described schematically in Fig. 1(a) are complementary to one another; the former is the end result of interference among coherent processes leading to a cancellation of the absorption cross section, while the latter emerges from the quantum interference of incoherent processes with the cancellation of the radiated fluorescence at certain frequencies and the appearance of a split spectrum.

We may also remark that, naively, one might interpret the appearance of a spectral hole as just a consequence of the Autler-Townes splitting of the upper state and the subsequent spontaneous emission from either one of the resulting levels. This argument ignores that the upper split states are phased together by the driving field, so that interference is unavoidable, and the process should really be interpreted as the spontaneous decay from dressed states. The shape of the emitted line and especially the appearance of a dark band in the middle of the spectrum, and the width of the two components (each half of which is predicted by the usual Weisskopf-Wigner theory, at least under resonant conditions) are symptoms of the essential role played by quantum interference in this spontaneous decay process.

ACKNOWLEDGMENTS

We would like to express our appreciation to Dr. P. L. Knight, Dr. Z. Y. Wang, and Dr. E. J. D'Angelo for helpful discussions and comments. We are especially indebted to Dr. J. H. Eberly and Dr. P. L. Knight for bringing to our attention earlier relevant studies of related processes. The work carried out by one of us (S.Y.Z.) was partially supported by the Research Grant Committee of the Hong Kong Government.

APPENDIX

The purpose of this appendix is to outline an alternative but equivalent approach to the one developed in Sec. II A for the calculation of the fluorescence spectrum in the upper level coupling scheme. By using dressed states as a basis, instead of bare atomic states, the origin of the interference effect becomes more transparent with only the minor drawback of some increase in computations. Furthermore, by adopting more general initial conditions, we demonstrate another surprising effect: it is possible to control the character of the interference process during the spontaneous emission, and force the system to display destructive or constructive interference, or other intermediate configurations.

We find this result surprising because, in view of the incoherent character of the decay, one would be tempted to assume that memory of the initial preparation should be lost. In fact, this is not the case, and the results, in a sense, are reminiscent of the double slit interference effect with a variable phase lag inserted in one of the slits.

For simplicity, we limit our analysis to the resonant case $\Delta_0=0$. The interaction Hamiltonian in the interaction picture has the same form as given by Eq. (2.6); now, however, we assume the state vector of the system at the arbitrary time t to have the form

$$|\Psi(t)\rangle=\sum_j C_{1j}(t)b_j^\dagger|\{0\}\rangle|1\rangle+\alpha(t)|\{0\}\rangle|\alpha\rangle + \beta(t)|\{0\}\rangle|\beta\rangle, \tag{A1}$$

where

$$|\alpha\rangle=\frac{1}{\sqrt{2}}(|2\rangle+ie^{i\varphi}|3\rangle) \tag{A2a}$$

and

$$|\beta\rangle=\frac{1}{\sqrt{2}}(|2\rangle-ie^{i\varphi}|3\rangle), \tag{A2b}$$

are the eigenstates of the Ω_0-dependent part of the Hamiltonian (2.6) (with $\Delta_0=0$), corresponding to the eigenvalues $+\hbar|\Omega_0|$ and $-\hbar|\Omega_0|$, respectively. The symbol φ is the phase of the driving field Ω_0 as in Eq. (2.25c).

As done in Sec. II A, our objective is to solve the Schrödinger equation (2.5) with the state vector given by Eq. (A1). For this purpose we must solve the coupled equations

$$\frac{d}{dt}C_{1j}(t)=-\frac{1}{\sqrt{2}}g_j e^{i\delta_j t}[\alpha(t)+\beta(t)], \tag{A3a}$$

$$\frac{d}{dt}\alpha(t)=-i|\Omega_0|\alpha(t)+\frac{1}{\sqrt{2}}\sum_j g_j C_{1j}(t)e^{-i\delta_j t}, \tag{A3b}$$

$$\frac{d}{dt}\beta(t)=i|\Omega_0|\beta(t)+\frac{1}{\sqrt{2}}\sum_j g_j C_{1j}(t)e^{-i\delta_j t}, \tag{A3c}$$

subject to the initial conditions $C_{1j}(0)=0$, $\alpha(0)=\alpha_0$, $\beta(0)=\beta_0$, where α_0 and β_0 are arbitrary complex numbers constrained only by the normalization condition

$$|\alpha_0|^2+|\beta_0|^2=1. \tag{A4}$$

At this point we follow the same procedure outlined in Sec. II; we solve formally for $C_{1j}(t)$, eliminate these variables from Eqs. (A3b) and (A3c), and apply the Weisskopf-Wigner approximation. Furthermore, it is convenient to introduce the new variables

$$X(t)=\alpha(t)+\beta(t), \tag{A5a}$$

$$Y(t)=\alpha(t)-\beta(t), \tag{A5b}$$

whose equations of motion take the simple form

$$\frac{dX(t)}{dt}=-i|\Omega_0|Y(t)-\tfrac{1}{2}\gamma X(t), \tag{A6a}$$

$$\frac{dY(t)}{dt}=-i|\Omega_0|X(t), \tag{A6b}$$

where the damping rate γ is given by Eq. (2.10c). It is now a simple matter to derive an explicit expression for the amplitudes $C_{1j}(t)$, whose form in the long-time limit becomes

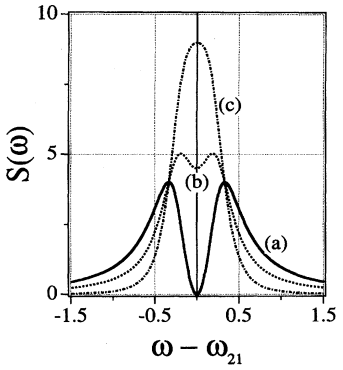

FIG. 9. Spontaneous emission spectrum $S(\omega)$ for the upper level coupling case for different initial atomic conditions and $\Omega_0=0.5$, $\Delta_0=0$; the three curves correspond to the following probability amplitudes for the atomic states 2 and 3: (a) $C_2=1$, $C_3=0$; (b) $C_2=C_3=1/\sqrt{2}$; (c) $C_2=0$, $C_3=1$.

$$C_{1j}(t\to\infty)=\frac{1}{\sqrt{2}}\frac{g_j}{s_1-s_2}\left[X_0\left(\frac{s_1}{s_1+i\delta_j}-\frac{s_2}{s_2+i\delta_j}\right)-i|\Omega_0|Y_0\left(\frac{1}{s_1+i\delta_j}-\frac{1}{s_2+i\delta_j}\right)\right], \tag{A7}$$

where

$$s_1=-\frac{\gamma}{4}+\left[\left(\frac{\gamma}{4}\right)^2-|\Omega_0|^2\right]^{1/2}, \tag{A8a}$$

$$s_2=-\frac{\gamma}{4}-\left[\left(\frac{\gamma}{4}\right)^2-|\Omega_0|^2\right]^{1/2}, \tag{A8b}$$

and

$$X_0=\alpha_0+\beta_0,\quad Y_0=\alpha_0-\beta_0. \tag{A9}$$

Note that Eq. (A7) reduces to Eq. (2.14c) if $\alpha_0=\beta_0=\sqrt{2}$ and $\Delta_0=0$. In general, however, the fluorescence spectrum which is still given by Eq. (2.18) differs from the one calculated in Sec. II A if one selects arbitrary initial conditions. In particular, for example, if the atom is excited initially in state $|3\rangle$, the initial values of the expansion amplitudes $\alpha(t)$ and $\beta(t)$ are given by

$$\alpha_0=-\frac{i}{\sqrt{2}}e^{-i\varphi}=-\beta_0, \tag{A10}$$

and the consequences of the quantum interference are very

different from before. We can check this statement at once if we calculate the central component of the spectrum, $S(\omega=\omega_{21})$, which in this case takes the value

$$S(\omega=\omega_{21})=\frac{1}{|\Omega_0|^2}. \tag{A11}$$

Thus, depending on the strength of the driving field Ω_0, the spectrum can exhibit a minimum or a maximum at the atomic transition frequency ω_{21}. Examples of the full spectral profile are shown in Fig. 9 for three different initial conditions and for the relatively weak Rabi frequency $\Omega_0=\gamma/4$.

[1] (a) U. Fano, Phys. Rev. **124**, 1866 (1961); (b) U. Fano and J. W. Cooper, Rev. Mod. Phys. **40**, 441 (1968).

[2] (a) D. Agassi, Phys. Rev. A **30**, 2449 (1984); (b) D. Agassi and J. H. Eberly, *ibid.* **34**, 2843 (1986); (c) P. M. Radmore, S. Tarzi, and P. L. Knight, J. Mod. Opt. **34**, 587 (1987); (d) S. Tarzi and P. M. Radmore, Phys. Rev. A **37**, 4734 (1988); (e) S. Tarzi, P. M. Radmore, and Stephen M. Barnett, J. Phys. B **22**, 2935 (1989); (f) P. L. Knight, *ibid.* **12**, 3297 (1979); (g) P. E. Coleman and P. L. Knight, *ibid.* **14**, 2139 (1981).

[3] (a) O. Kocharovskaya and Ya. I. Khanin, Pis'ma Zh. Eksp. Teor. Fiz. **48**, 581 (1988) [JETP Lett. **48**, 630 (1988)]; (b) S. E. Harris, Phys. Rev. Lett. **62**, 1033 (1989); (c) M. O. Scully, S.-Y. Zhu, and A. Gavrielides, *ibid.* **62**, 2813 (1989); (d) O. Khocharovskaya and P. Mandel, Phys. Rev. A **42**, 523 (1990); (e) L. M. Narducci, H. M. Doss, P. Ru, M. O. Scully, S.-Y. Zhu, and C. H. Keitel, Opt. Commun. **81**, 379 (1991).

[4] (a) S. E. Harris, J. E. Field, and A. Imamoglu, Phys. Rev. Lett. **64**, 1107 (1990); (b) K. J. Boller, A. Imamoglu, and S. E. Harris, *ibid.* **66**, 2593 (1991); (c) J. E. Field, K. H. Hahn, and S. E. Harris, *ibid.* **67**, 3062 (1991); (d) K. Hakuta, L. Marmet, and B. P. Stoicheff, *ibid.* **66**, 596 (1991).

[5] (a) M. O. Scully, Phys. Rev. Lett. **67**, 1855 (1991); (b) M. O. Scully and S.-Y. Zhu, Opt. Commun. **87**, 134 (1992).

[6] See, for example, M. O. Scully and M. Fleischhauer, Phys. Rev. Lett. **69**, 1360 (1992).

[7] See, for example, (a) G. Alzetta, A. Gozzini, L. Moi, and G. Orriols, Nuovo Cimento B **36**, 5 (1976); (b) H. R. Gray, R. M. Whitley, and C. R. Stroud, Jr., Opt. Lett. **3**, 218 (1978).

[8] Here we consider a situation that should not be confused with the ordinary resonance fluorescence, where the driving field couples only the two levels that are responsible for the fluorescent emission.

[9] S. H. Autler and C. H. Townes, Phys. Rev. **100**, 703 (1995).

[10] There are numerous demonstrations of this effect. See, for example, D. E. Nitz, A. V. Smith, M. D. Levenson, and S. J. Smith, Phys. Rev. A **24**, 288 (1981).

[11] Whether level 3 has a higher or lower energy than level 2 is immaterial for our purposes. In practice, however, it is preferable for level 3 to be higher lying in order to avoid complications connected with the existence of an alternative decay pathway for level 2.

[12] (a) L. M. Narducci, M. O. Scully, G.-L. Oppo, P. Ru, and J. R. Tredicce, Phys. Rev. A **43**, 3748 (1991); (b) A. S. Manka, H. M. Doss, L. M. Narducci, P. Ru, and G.-L. Oppo, *ibid.* **43**, 3748 (1991).

[13] (a) V. Weisskopf and E. Wigner, Z. Phys. **63**, 54 (1930); (b) **65**, 18 (1931).

[14] C. H. Keitel, P. L. Knight, L. M. Narducci, and M. O. Scully, Opt. Commun. **118**, 143 (1995). This work considers the spontaneous emission of excited two-level atoms in a resonator and under the action of a driving field. Unlike the conventional approach, the authors consider first the exact interaction of the atom with the driving field, and then the effect of the surrounding vacuum within the Weisskopf-Wigner approximation, as done also in this section. The conventional and the dressed atom approaches are not equivalent, but in empty space their differences are entirely negligible by virtue of the weak frequency dependence of the vacuum density of states [see Eqs. (2.30a) and (2.30b) in the present paper].

[15] (a) M. Lax, Phys. Rev. **172**, 350 (1968); (b) H. Haken and W. Weidlich, Z. Phys. **205**, 96 (1967); (c) M. Lax, in *Statistical Physics, Phase Transitions, and Superfluidity*, edited by M. Chretien, E. P. Gross, and S. Deser (Gordon and Breach, New York, 1968), Vol. 2, p. 265.

[16] We note that the extended version of the model illustrated in Fig. 1(a) is, in fact, identical to the cascade system studied in Ref. [12(b)]. At the time when this paper was prepared for publication, we were not aware of the dark-line feature of the fluorescence spectrum, nor of its possible significance. For the parameter values used in Ref. [12(b)] the effect is not observable. Furthermore, the analytic expressions developed in Sec. VI of Ref. [12(b)] are not helpful because they are valid only in the limit of a large effective Rabi frequency, while the interference effects of interest in this work are especially pronounced when the Rabi frequencies of the applied fields are not too large, e.g., comparable to the incoherent relaxation rates W_{ij} (see, for example, Fig. 7 of this work).

[17] (a) V. F. Cheltsov, Zh. Eksp. Teor. Fiz. **48**, 1139 (1965) [Sov. Phys. JETP **21**, 761 (1965)]; (b) M. C. Newstein, Phys. Rev. **167**, 89 (1969); (c) B. R. Mollow, *ibid.* **188**, 1969 (1969); (d) B. R. Mollow, Phys. Rev. A **2**, 76 (1970).